MOLECULAR IMAGING AND BIOLOGY

Mol Imaging Biol (2019) 21:482–490
DOI: 10.1007/s11307-018-1269-9

Published Online: 5 September 2018

RESEARCH ARTICLE

Spatial Inhomogeneity of Cardiac Norepinephrine Transport Protein and Meta-[^{123}I]Iodobenzylguanidine Uptake in Swine Myocardial Tissue

Claudia Kusmic,[1] Assuero Giorgetti,[2] Cristina Barsanti,[1] Silvia Burchielli,[2] Debora Petroni,[1] Annette Kusch,[2] Dario Genovesi,[2] Luca Menichetti,[1,2] Paolo Marzullo[1,2]

[1]*Institute of Clinical Physiology, Consiglio Nazionale delle Ricerche (CNR), Via Moruzzi, 1, 56124, Pisa, Italy*
[2]*Fondazione Toscana G. Monasterio, Via Moruzzi, 1, 56124, Pisa, Italy*

Abstract

Purpose: The aim of the present study was to evaluate the expression of the cardiac norepinephrine transporter (NET) in the left ventricle (LV) of healthy pigs and its relationship with regional meta-[^{123}I]iodobenzylguanidine ([^{123}I]MIBG) myocardial uptake.

Procedures: Experiments were performed on animals injected with [^{123}I]MIBG and acquired 2 h later using an ultrafast CZT gamma camera to assess the regional myocardial uptake. After image acquisition, animals were euthanized; the heart was quickly excised and underwent to an *ex vivo* single photon emission tomography (SPECT) imaging. Four small samples of tissue were then harvested from mid-walls and apex of the left ventricle; NET densities were evaluated and further normalized for protein loading per cardiac region.

Results: Three variants of NET protein with different molecular weights were detected. The expression of NET was not homogenous in the LV, with the highest density in the inferior wall and the lowest one in the apical area. The regional *in vivo* [^{123}I]MIBG uptake revealed an analogous trend, showing a good linear relationship with NET expression. Parallel results were obtained from the *ex vivo* study.

Conclusion: This study elucidates the expression of three different variants of NET proteins into the left ventricular myocardium of a healthy pig. NET expression into the LV was not homogeneous and paralleled by differences in regional [^{123}I]MIBG uptake. Moreover, the correlation and the agreement between measurements of regional expression of NET variants and [^{123}I]MIBG uptake represent a relevant finding for inferences about NET expression in the context of clinical imaging.

Key words: NET, [^{123}I]MIBG, CZT, Cardiac sympathetic innervation, Ultrafast cardiac camera

Introduction

Norepinephrine is the main neurotransmitter released from post-ganglionic sympathetic neurons in peripheral tissue. Approximately 80–90 % of the norepinephrine released in the

Correspondence to: Claudia Kusmic; *e-mail:* kusmic@ifc.cnr.it, Assuero Giorgetti; *e-mail:* asso@ftgm.it

synaptic cleft is taken up again through the neuronal norepinephrine transporter (NET). The re-uptake process is an ATP-dependent transport, originally termed *uptake-1* [1]. NET belongs to the monoamine transporter family with a predicted topological structure of 12 membrane spanning domains [2]. Based on the level of glycosylation, three molecular weight variants of human NET have been identified by immunoblotting transfected cell line [3, 4]. The presence of one or more NET protein variants, as along slight specie-specific variations in the molecular weight within each variant, were described in different cells or native tissues [5–8].

NET function is considered the molecular prerequisite for the noninvasive investigation of cardiac adrenergic innervation *in vivo* by means of radiotracers employed in nuclear medicine, such as [^{123}I]meta-iodobenzylguanidine ([^{123}I]MIBG), that is assumed to follow the molecular pathway of norepinephrine *via* the *uptake-1* [9].

Previous clinical single photon emission tomography (SPECT) studies with [^{123}I]MIBG have demonstrated significant impairments in cardiac sympathetic innervation in patients with heart failure, diabetic cardiac autonomic neuropathy, and Parkinson's disease [10–14].

More recently, several experimental studies on rodents demonstrated that the reduced myocardial [^{123}I]MIBG uptake observed in type 2 diabetes and Parkinson's disease models was associated with a decrease in NET density [15–19]. Conversely, there are few and sometimes discordant data on the regional homogeneity of [^{123}I]MIBG accumulation and NET density in the left ventricle (LV) of healthy hearts. Indeed, in 2002, Kyono and coworkers reported a difference in [^{123}I]MIBG uptake paralleled by a different NET density between anterior and inferior LV walls in control rats [15, 18]. However, this result was not confirmed in a later study, in which the same authors reported no significant difference between anterior and inferior walls in the same animal model [20].

Despite the extensive clinical use of [^{123}I]MIBG cardiac imaging, there is still a lack of information about the functional relationship between radiotracer uptake and regional NET expression into the LV.

To improve the knowledge about this topic, the present study has been developed with the dual aim to (i) evaluate which of the NET isoforms and with what extent they are expressed in the left ventricular myocardium of pigs, and (ii) characterize the regional myocardial distribution of [^{123}I]MIBG in association with regional myocardial blood flow and NET expression.

Materials and Methods

All regulatory aspects for laboratory animal care were followed; the study was performed fully in accordance with the European Directive (2010/63/UE) and the Italian law (D.L 26/2014). The study was approved by the Ethical Committee of Experimental Biomedicine Centre, National Research Council, Pisa, Italy, and by the competent national authority (Italian Ministry of Health).

Animals

Eight young healthy castrated farm pigs (weight 32–41 kg, mean 37 ± 4 kg) were used in the study. Two animals were dedicated in a pilot study to characterize the expression of the swine NET isoforms in the three layers (epicardium, midcardium, and endocardium) of LV full-thickess cardiac wall (Fig. 1b).

Indeed, transmural tissue collection, differently to subepicardial sampling, involves the presence of holes that could compromise the imaging acquisition.

Six pigs underwent LV myocardial perfusion/function and sympathetic innervation study. After sacrifice, the epicardial tissue was harvested with due precautions from predefined different regions of LV (Fig. 1a); SPECT imaging procedure was previously developed by us [21]. Briefly, animals were fasted for 12 h without any limitation in drinking water and then were pre-anesthetized *via* intramuscular administration of a solution composed by Zoletil®, Atropine, and Stresnil® (10, 0.1, and 2 mg/kg, respectively). One bolus of 2 mg/kg of Propofol was intravenously injected in the marginal ear. Animals were ventilated *via* an endotracheal cannula with pure oxygen at a respiratory rate of 15 cycles/min and a tidal volume of 10–15 ml/kg. The continuous infusion of 5–8 mg/kg/h of Propofol maintained the adequate grade of anesthesia throughout the experimental session.

The respiratory parameters were timely verified and eventually adjusted to maintain the pH 7.35–7.45, pCO_2 35–45 mmHg, and pO_2 > 120 mmHg. Four conducting plates were positioned at the animal legs for monitoring heart rate and for ECG-gating recordings. The adequate depth of anesthesia and sedation were periodically checked by tail-clamping, corneal reflex, and the presence of lacrimation, and the main physiological parameters (temperature, blood pressure, and heart rate) were continuously monitored.

CZT Scintigraphic Imaging

Left ventricular myocardial perfusion/function was assessed using [^{99m}Tc]tetrofosmin (26 ± 6 MBq) and a CZT camera (Discovery NM530c; GE Healthcare) [21]. Briefly, two experienced nuclear cardiologists independently performed a semiquantitative analyses of regional myocardial perfusion, using a 17-segment model of the left ventricle (LV) and a five-point scale (0 = normal, 1 = mild, 2 = moderate, 3 = severe reduction of radioisotope uptake, and 4 = absence of detectable tracer uptake) and in cases of disagreement, consensus was reached.

Semiquantitative gated SPECT was performed at rest and the parameters of ejection fraction (EF%), end-diastolic volume (EDV, ml), and end-systolic volume (ESV, ml) were calculated. A normal perfusion/function imaging was set as the inclusion criteria before to proceed to the innervation study.

Myocardial innervation was imaged with [^{123}I]MIBG (54 ± 14 MBq). Tomographic acquisitions in list mode were obtained

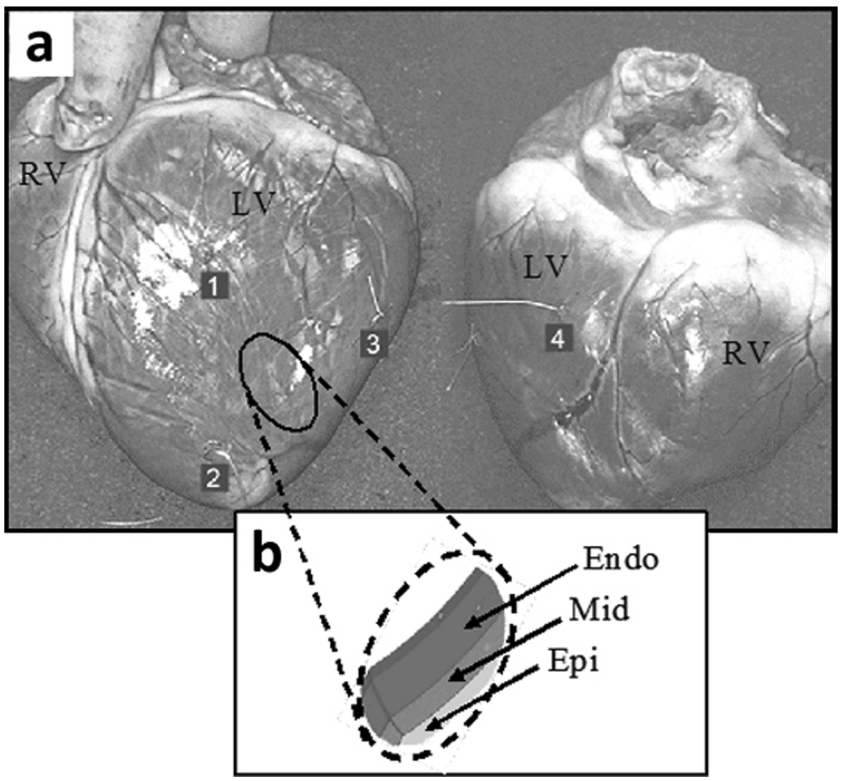

Fig. 1. Picture illustrating the explanted pig heart. **a** Sampling of LV myocardium in 1 = mid-anterior wall; 2 = apical wall; 3 = mid-lateral wall; and 4 = mid-inferior wall. RV, right ventricle; LV, left ventricle. **b** Enlargment of the oval in **a** detailing the full-thickness wall sampling and the separation in the three myocardial layers: Epi, epicardium; Mid, mid-myocardium; Endo, endocardium.

at 2 h following the radiotracer injection for a duration of 10 min. Then, SPECT data were reconstructed using a dedicated maximum penalized likelihood expectation maximization iterative algorithm (50 iterations; regularization type: OSL green; MAP parameters: Green OSL Alpha 0.41, Green OSL Beta 0.2) and a 10 % energy window centered at the photopeak of I-123 (159 keV ± 5 %). A Butterworth post-processing filter (frequency 0.37, order 7) was applied to the reconstructed slices. The tomographic studies were also re-projected into 60 planar projections. Images were reconstructed without scatter or attenuation correction. Regional myocardial distribution of radiotracer, expressed as mean counts per voxel/min (cpm), was obtained by means of Corridor 4DM-SPECT software and reported into a 13-segment bull's-eye projection. Then, regional [^{123}I]MIBG uptake was corrected for radiotracer decay and alternatively normalized for either the maximum activity ([^{123}I]MIBG % uptake) into the LV or for the injected dose.

Ex Vivo Cardiac Tissue Harvesting and CZT Innervation SPECT Study

Immediately after the *in vivo* imaging session, pigs were euthanized by injecting a lethal dose of KCl and underwent thoracotomy: the heart was quickly excised, placed on ice, and the blood completely drained. Before proceeding with the *ex vivo* cardiac innervation study, four small samples were harvested from predefined LV regions (Fig. 1a).

Densitometric analysis of bands from the pilot study, showing a comparable expression of NET through the wall thickness of left ventricle, highlighted the interchangeability of layers. Thus, to preserve muscle integrity for SPECT *ex vivo* acquisition, in imaged pigs, myocardial tissues were probed from subepicardial territory only. Tissue samples were weighed for recording, snap frozen in liquid nitrogen, and stored at − 80 °C until use. Then, the left ventricular cavity of the explanted hearts was filled, through the mitral orifice, with inert soft material to preserve its shape. An *ex vivo* SPECT acquisition in list mode (10 min lasting) was performed using the CZT gamma camera and myocardial images were reconstructed and analyzed following the same protocol used in the *in vivo* imaging.

Western Blot Analysis of NET Expression

The full-thickness samples of LV wall collected at sacrifice of the two dedicated pigs were sectioned to obtain three distinct layers: epicardium, mid-myocardium, and endocardium. The epicardial samples were collected from the six pigs undergone SPECT studies, between the *in vivo* and *ex vivo* acquisition. All the samples were promptly frozen in

liquid nitrogen and stored at − 80 °C until use. Frozen cardiac tissues of all animals were cut into small pieces and homogenized by Tissue Lyser (Qiagen®), two cycles of 2 min at 25 Hz, in buffer containing 10 mM HEPES, 0.15 M NaCl, 1 mM EDTA, and 1 mM PMSF (pH 7.4), with the addition of protease and phosphatase inhibitors. After centrifugation at 700×*g* for 5 min at 4 °C, the supernatants were collected and quantified for total protein concentration with BCA protein assay kit (Pierce, Thermo Fisher Scientific Inc., Rockford, IL). Samples were then diluted in loading buffer and resolved (25 µg/lane) on 10 % SDS-PAGE electrophoresis gels. After protein transferring onto PVDF, the membranes were blocked with 5 % nonfat dry milk for 2 h and incubated overnight at 4 °C with anti-norepinephrine transporter rabbit polyclonal antibody (#AB2234, Millipore), or with anti-HPRT (hypoxanthine-guanine phosphoribosyltransferase) mouse monoclonal antibody diluted 1:10000 (#T5168, Sigma-Aldrich) as reference protein. The membranes were then rinsed and incubated with the secondary antibodies (anti-rabbit HRP #7074 or anti-mouse HRP #7076, Cell Signaling Technology®). The immunoreactivity was detected using LiteAblot® Extend chemiluminescent substrate (EuroClone), and after image acquisition, densitometric analysis of bands was performed with the ImageJ analysis software (NIH, Bethesda, MD, USA). Normalized densities by the reference protein were further normalized for protein loading per cardiac region.

Statistical Analysis

Continuous variables are presented as mean ± standard deviation. Where indicated, differences were assessed by Student's *t* test for paired or unpaired data. Differences in myocardial [^{123}I]MIBG uptake both *in vivo* and *ex vivo* and NET expression in different segments of the LV were compared by ANOVA with the Bonferroni *post hoc* test. The significance of the relationship between regional NET expression and [^{123}I]MIBG uptake was assessed by linear regression analysis. Analysis of agreement was also performed by means of the Bland–Altman method [22]. A value of $p < 0.05$ was considered statistically significant. Statistical analysis was performed using SPSS Version 23 (IBM, New York, NY, USA) software.

Results

NET Protein Expression in the LV

Three molecular weight variants of NET protein were detected in all three layers of the full-thickness wall (Fig. 1a, b): 80, 54, and 41 kDa (Fig. 2).

Quantitative analysis showed that the ratio of expression of the 80 kDa form was 2.9-fold and 5.5-fold over the 54 and 41 kDa forms of protein, and the level of 54 kDa variant was 1.9-fold higher than 41 kDa form, independent of the myocardial layer of the LV wall (Fig. 2).

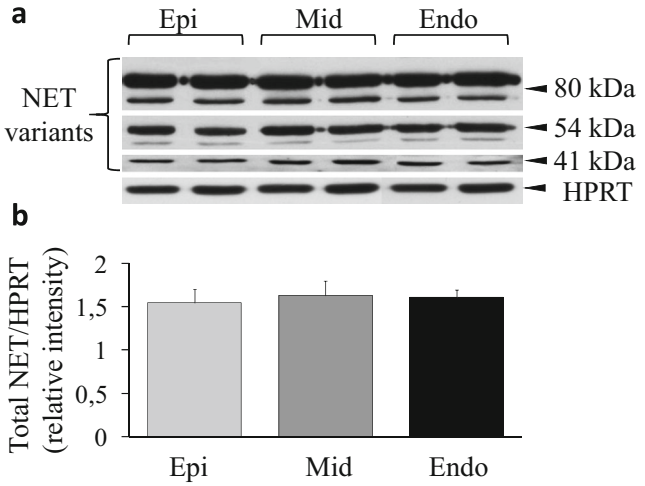

Fig. 2. **a** Representative Western blots of the three forms of NET with molecular weight of about 80, 54, and 41 kDa, expressed in the LV of pig heart. HPRT was used as reference protein. **b** Quantitative results from densitometric analysis of total NET relative expression in the epicardial (Epi), mid-myocardial (Mid), and endocardial (Endo) tissue samples. Each sample was analyzed in triplicate ($n = 2$ pigs).

In addition, densitometric analysis of bands showed comparable results among NET protein detected in epicardial, mid-myocardial, and endocardial layers (Fig. 2b). This result allows to generalize with confidence the findings observed in the subepicardial tissues (sampled in pigs subjected SPECT imaging and showed in Fig. 3a) in respect to the transmural myocardial thickness.

The expression of total NET (41, 54, and 80 kDa) was not homogenous among the LV regions (Fig. 3), with the highest density in the inferior wall ($p < 0.001$ *vs* apical wall and $p = 0.001$ *vs* anterior wall; $p = 0.055$ *vs* lateral wall) and the lowest one in the apical area ($p < 0.001$ *vs* inferior wall; $p < 0.05$ *vs* lateral wall).

Similar results were also achieved by a separate analysis for each of the two main variants of NET, but not for the 41 kDa form of the protein. In addition, a positive correlation of 80 kDa *vs* 54 kDa or 41 kDa forms was found ($y = 2.65 + 0.9x$; $r = 0.66$, $p < 0.001$ and $y = 28.13 + 0.61x$; $r = 0.48$, $p = 0.01$, respectively). Conversely, no correlation was found between 54 and 41 kDa ($r = 0.144$, $p =$ ns).

Left Ventricular Myocardial Perfusion/Function

All pigs showed normal myocardial perfusion and function, as previously described [21]. Briefly, the mean [^{99m}Tc]tetrofosmin summed rest score was 2.6 ± 1.5 (range, 0–4), EF% was 63.8 ± 4.7, EDV was 48.8 ± 7.3 ml, and ESV was 16.5 ± 2.4 ml. A representative SPECT image sample of regional distribution of short axis left ventricle is showed in Fig. 4.

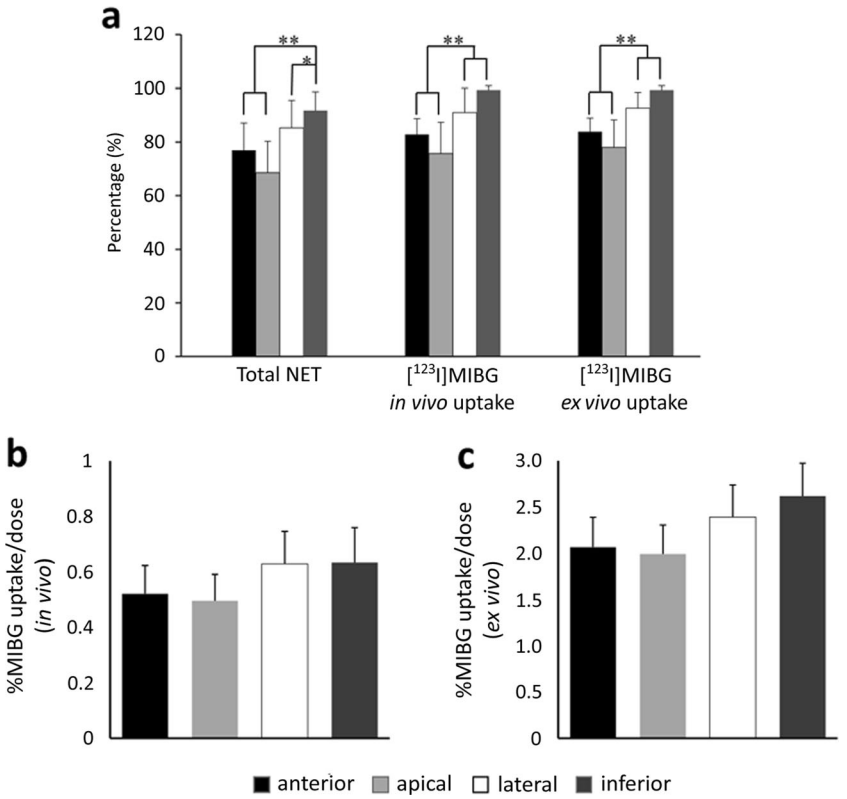

Fig. 3. **a** Multiple variables graph illustrating regional NET expression, [^{123}I]MIBG percentage uptake *in vivo* and *ex vivo* in the different regions sampled in the LV. Different variables showed an inhomogeneous distribution among the sampled regions of LV; a similar trend emerges among the variables studied (*$p < 0.05$; **$p \leq 0.001$). **b** *In vivo* regional [^{123I}]MIBG percentage uptake/dose in the different LV regions sampled. **c** *Ex vivo* regional [^{123I}]MIBG percentage uptake/dose in the different LV regions sampled. The inhomogeneous profile of radiotracer uptake among the sampled regions is reflected in all the three panels. Data are reported as mean ± SD ($n = 6$ pigs).

In Vivo Regional [^{123}I]MIBG % Uptake vs Regional NET Protein Expression

Regional percentage uptake of [^{123}I]MIBG was not homogeneous in the LV and paralleled with NET protein expression (Fig. 3). *In vivo* [^{123}I]MIBG normalized uptake resulted 83 ± 6 % in the anterior wall ($p < 0.001$ *vs* inferior and lateral), 76 ± 11 % in the apex ($p < 0.001$ *vs* inferior and lateral), 91 ± 9 % in the lateral wall, and 99 ± 1 % in the inferior wall. A similar trend is evident by expressing the percentage of [^{123}I]MIBG % uptake per dose (Fig. 3b). However, in this case, due to the large intersubject variability, the difference in regional MIBG uptake did not reach the statistical significance. The regional *in vivo* [^{123}I]MIBG uptake showed a good correlation with the expression of the NET protein whether had been normalized for the maximum activity ($y = 24.86 + 0.778x$, $r = 0.846$, $p < 0.001$) (Fig. 5a) or for the injected dose ($y = -0.074 + 0.166x$, $r = 0.538$, $p < 0.01$) (Fig. 5c).

The Bland–Altman analysis confirmed a good agreement between the two measures in case they were expressed in the same dimension, *i.e.*, normalized to their regional maximum (mean difference −6.6 ± 6.9 %), with 96 % of the results within the limits of agreement (−20.1 to 7.0 %) (Fig. 5b).

Ex Vivo Regional [^{123}I]MIBG % Uptake vs Regional NET Protein Expression

The *ex vivo* regional % uptake of [^{123}I]MIBG resulted not homogeneous in the LV (Fig. 3a). [^{123}I]MIBG uptake was 84 ± 5 % in the anterior wall ($p < 0.001$ *vs* inferior and lateral), 78 ± 10 % in the apex ($p < 0.001$ *vs* lateral and inferior), 93 ± 5 % in the lateral wall, and 99 ± 2 % in the inferior wall. A similar profile was observable by expressing the percentage of [^{123}I]MIBG % uptake per dose (Fig. 3c). Likewise to *in vivo* data, however, the difference in regional [^{123}IMIBG uptake did not reach the statistical significance. Regional [^{123}I]MIBG % uptake normalized at both maximum activity or dose showed an excellent correlation with NET protein expression ($y = 15.96 + 0.86x$, $r = 0.849$, $p < 0.001$ for MIBG % uptake/max; $y = -0.392 + 0.684x$, $r = 0.714$, $p < 0.001$ for MIBG % uptake/dose) as shown in Fig. 6a and Fig. 6c, respectively.

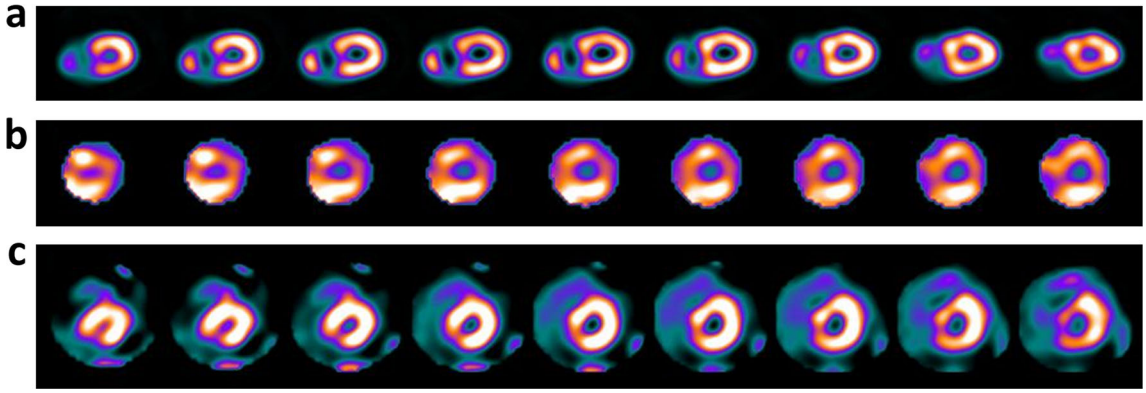

Fig. 4. A SPECT pictures representative sample of short axis left ventricle (pig#3) of regional perfusion with [^{123}I]MIBG and [^{99m}Tc]tetrofosmin. **a** *In vivo* view [^{99m}Tc]tetrofosmin perfusion imaging. **b** *In vivo* view [^{123}I]MIBG imaging. **c** *Ex vivo* view [^{123}I]MIBG imaging on explanted heart.

The Bland–Altman analysis confirmed a good agreement between the two measures using [^{123}I]MIBG % uptake/max (mean difference -5.04 ± 7.1 %) with 92 % of the results within the limits of agreement (-19.0 to 8.9 %) (Fig. 6b).

Discussion

NET Protein Expression in the LV of Healthy Pigs

To date, limited and sparce data are available on the expression of NET variants in experimental models and in particular in porcine myocardial tissue. In our study, we found that the LV in healthy pigs expresses three isoforms of NET protein, namely 80, 54, and 41 kDa forms. The three molecular weight variants of NET have been described on the basis of the level of their glycosylation grade: the 80 kDa form is generally considered the functional, fully glycosylated form exposed on surface membranes; the 54 kDa is the partially glycosylated intermediate and its functional role in norephinephrine transport or trafficking is still debated [5]. Conversely, the low molecular weight variant (correspondent to 41 kDa in pig samples) is the immature core protein with a very short half-life, and the available information leads to exclude any functional role [3]. Despite slight variations in the molecular weight within each variant, the present finding is in agreement with previous observation obtained in different animal species [5–8] and in human beings [3, 4]. In the absence of certain evidence on the real function of all the three forms of the protein, in our study, we considered both the sum of all the variants (total NET) and the individual variants to express our results. However, given the relative abundance of the variants observed, the influence of the contribution of the variant 41 kDa in the calculation of total NET is definitely lower than the other two (80 and 54 kDa), independently of its actual functional role.

By sampling different areas of the left ventricle, we uncovered a significant difference in the regional expression of total NET protein, with the highest levels in the the inferior wall and the lowest levels in the apex. Similarly, the distribution of post-ganglionic symphatethic fibers into LV is known to be heterogeneous in the dog, with a prevalent innervation of the anterior and lateral wall [23]. Moreover, a significant gradient in noreephinephrine concentration has been observed, with a significant decrease from base to apex, in the ventricles of primates [24]. In our study, the molecular evaluation by means of Western blot analysis allowed to discriminate between the NET variants, providing additional information about the homogeneity of distribution of the individual isoforms. Interestingly, only for the 41 kDa variant, the one supposed without any functional role, the distribution did not differ among the four cardiac regions analyzed. This outcome deserves a further dedicated

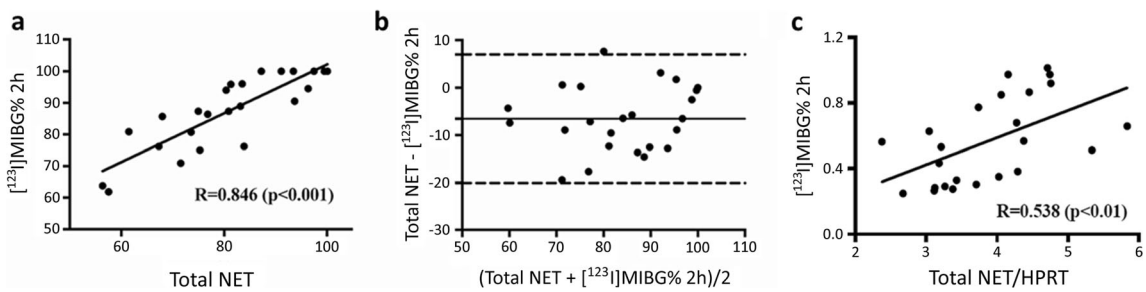

Fig. 5. **a** Linear relationship between regional NET expression and [^{123}I]MIBG % *in vivo* uptake normalized to its maximum activity. **b** The Bland–Altman analysis of data presented in (**a**) showed an excellent agreement between the two measures. **c** Linear relationship between regional NET expression and [^{123}I]MIBG % *in vivo* uptake normalized to the injected dose.

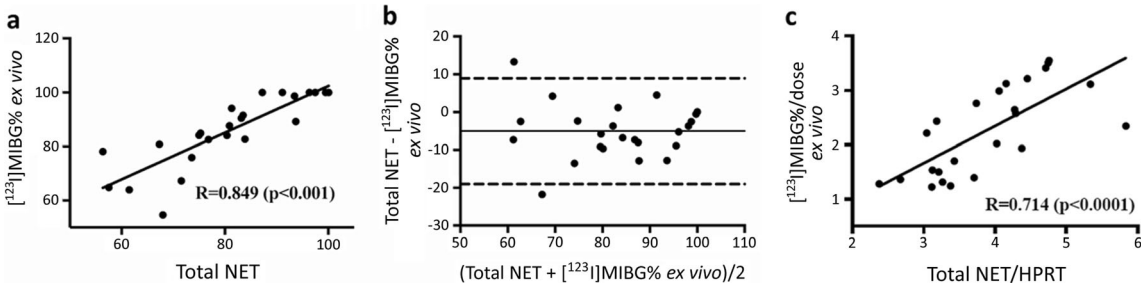

Fig. 6. **a** Linear relationship between regional NET expression and [^{123}I]MIBG % uptake normalized to its maximum activity in the explanted heart. **b** The Bland–Altman analysis of data presented in (**a**) showed an excellent agreement between the two measures. **c** Linear relationship between regional NET expression and [^{123}I]MIBG % *ex vivo* uptake normalized to the injected dose.

investigation to get light on the issue of the NET isoforms, their different degrees of glycosilation, protein maturation, and function, in view of their different regional distributions in the myocardium.

In Vivo and Ex Vivo Regional [^{123}I]MIBG % Uptake vs Regional NET Protein Expression

A good agreement between the *in vivo* and *ex vivo* acquisitions has been achieved mainly due to the improved sensitivity and spatial resolution of CZT cardiac-dedicated SPECT camera. By sampling different areas of the LV, we found an inhomogeneous distribution of NET protein with lowest values in the apical wall and the highest in the inferior one. *Ex vivo* data resulted in a closer agreement with NET expression, as shown by statistics (lower mean difference and narrowed confidence interval), than *in vivo* data. These results could be attributed by reduced interference by radioactive blood pool and partial volume effect in explanted heart. The persistent linear dependence between tracer uptake and the molecular density of NET independently of the way of data normalization suggested the [^{123}I]MIBG retention as a good surrogate to measure NET expression in the heart. Moreover, the observed agreement could provide new insights for understanding the pattern of distribution of myocardial [^{123}I]MIBG uptake in healthy hearts. Indeed, data on regional distribution of the radiotracers into the LV are scarce and dated. Some authors reported that [^{123}I]MIBG uptake is lower in the inferior and septal than in the anterior and lateral walls [25, 26]. Three mechanisms have been proposed for the heterogeneous [^{123}I]MIBG distribution: variation in sympathetic innervation, attenuation by the diaphragm, and artifact defect created by high counts into the liver. Likely, all the three mechanisms can play a role in determining an inhomogeneous radiotracers uptake but it should be noted that heterogeneity is a physiological phenomenon in cardiology, as in the case of regional myocardial blood flow distribution and LV contractility.

In this study, we found the inferior wall of LV with the highest expression of the NET proteins paralleled by the highest [^{123}I]MIBG uptake. This finding is partially in agreement with previous observation obtained with prone imaging [27] and with [^{11}C]hydroxyephedrine by positron emission tomography [28].

In addition, the use of an ultrafast cardiac gamma camera, with a high spatial resolution, can have minimized artifacts often observed with conventional SPECT systems. On the other hand, the lowest uptake observed in the apex could represent a physiological lower density of the sympathetic nerves in this region with the lowest myocardial thickness.

Study Limitations

Some limitations of our study have been analyzed, including the sample size. In our view, this work represents a feasibility study for the assessment of regional NET protein expression in healthy pigs. Further studies need to be addressed both in physiological and pathological conditions in the same model to extend our results to human beings.

Also, the acquisition protocol, limited to 125 min, could be criticized. However, most of the studies in literature have acquisition protocols quite similar. Prolonging the time of acquisition, especially in experimental studies on anesthetized animals, might impair the physiological and hemodynamic parameters, increasing the possibility to introduce confusing results. The comparison between the anatomical samples and regional SPECT segments could be less than perfect. However, we obtained similar results in the distribution of the studied variables. Moreover, it has been reported that anesthetics can affect tracer uptake [29] and fluctuations in their plasma levels could have had an effect on the obtained results. Furthermore, since we did not account for differences in catecholamine activation among the animals, it is difficult to draw any conclusion on the individual variability in tracer uptake.

Clinical Implications

Myocardial innervation scintigraphy has been demonstrated to be a potent prognostic imaging tool in patients with cardiac disease [1]. Despite its recognized clinical utility, the use of [^{123}I]MIBG cardiac scintigraphy is still

underestimated considering the putative information provided by the radiotracer. Indeed, the few quantitative parameters provided to clinicians are usually limited to global indexes (heart to mediastinum analysis and washout rate evaluation). However, even with a SPECT approach, important supplementary information and additional features can be achieved by serial planar imaging. The demonstration of a close relationship between regional NET protein expression and [^{123}I]MIBG uptake is a basic prerequisite to use cardiac innervation scintigraphy for characterizing the myocardium in terms of catecholamine kinetic. Regional distribution of sympathetic innervation, alone or matched with regional myocardial perfusion, could be relevant to clinicians to discriminate the pathophysiological mechanisms underlying different myocardial diseases and to provide personalized therapeutic interventions.

Conclusions

Our study provides an original outlook about regional expression of NET and the regional [^{123}I]MIBG uptake into the LV myocardium of a porcine experimental model. Results confirmed previous observations obtained in different species demonstrating the expression of three different variants of NET proteins in healthy pigs. The demonstration of expression of NET isoforms in porcine heart and the agreement with previous observations in human beings could have important research implication, in particular in extending data obtained in experimental preparation toward the comprehension of the regional function of human NET. Moreover, the correlation between regional NET expression and [^{123}I]MIBG uptake represents a relevant finding for the assessment of NET expression in the context of clinical imaging.

Compliance with Ethical Standards. All regulatory aspects for laboratory animal care were followed; the study was performed fully in accordance with the European Directive (2010/63/UE) and the Italian law (D.L 26/2014). The study was approved by the Ethical Committee of Experimental Biomedicine Centre, National Research Council, Pisa, Italy, and by the competent national authority (Italian Ministry of Health).

Conflict of Interest

The authors declare that they have no conflict of interest.

References

1. Schroeder C, Jordan J (2012) Norepinephrine transporter function and human cardiovascular disease. Am J Physiol Heart Circ Physiol 303:H1273–H1282
2. Bonisch H, Runkel F, Roubert C et al (1999) The human desipramine-sensitive noradrenaline transporter and the importance of defined amino acids for its function. J Auton Pharmacol 19:327–333
3. Melikian HE, McDonald JK, Gu H, Rudnick G, Moore KR, Blakely RD (1994) Human norepinephrine transporter. Biosynthetic studies using a site-directed polyclonal antibody. J Biol Chem 269:12290–12297
4. Melikian HE, Ramamoorthy S, Tate CG, Blakely RD (1996) Inability to Nglycosylate the human norepinephrine transporter reduces protein stability, surface trafficking, and transport activity but not ligand recognition. Mol Pharmacol 50:266–276
5. Bruss M, Porzgen P, Bryan-Lluka LJ, Bonisch H (1997) The rat norepinephrine transporter: molecular cloning from PC12 cells and functional expression. Brain Res Mol Brain Res 52:257–262
6. Burton LD, Kippennerger AG, Lingen B et al (1998) A variant of the bovine noradrenaline transporter reveals the importance of the C-terminal region for correct targeting to the membrane and functional expression. Biochem J 330:900–914
7. Palomar AR, Larios BN, De Sanchez VC et al (2011) Expression and distribution of dopamine transporter in cardiac tissues of the guinea pig. Neurochem Res 36:399–405
8. Wehrwein EA, Parker LM, Wright AA, Spitsbergen JM, Novotny M, Babankova D, Swain GM, Habecker BA, Kreulen DL (2008) Cardiac norepinephrine transporter protein expression is inversely correlated to chamber norepinephrine content. Am J Physiol Regul Integr Comp Physiol 295:R857–R863
9. Travin MI (2013) Cardiac autonomic imaging with SPECT tracers. J Nucl Cardiol 20:128–143
10. Kreiner G, Wolzt M, Fasching P, Leitha T, Edlmayer A, Korn A, Waldhausl W, Dudczak R (1995) Myocardial m-[^{123}I]iodobenzylguanidine scintigraphy for the assessment of adrenergic cardiac innervation in patients with IDDM. Comparison with cardiovascular reflex tests and relationship to left ventricular function. Diabetes 44:543–549
11. Hattori N, Tamaki N, Hayashi T et al (1996) Regional abnormality of iodine-123-MIBG in diabetic hearts. J Nucl Med 1996(37):1985–1990
12. Yoshita M (1998) Differentiation of idiopathic Parkinson's disease from striatonigral degeneration and progressive supranuclear palsy using iodine-123 meta-iodobenzylguanidine myocardial scintigraphy. J Neurol Sci 155:60–67
13. Satoh A, Serita T, Seto M, Tomita I, Satoh H, Iwanaga K, Takashima H, Tsujihata M (1999) Loss of ^{123}I-MIBG uptake by the heart in Parkinson's disease: assessment of cardiac sympathetic denervation and diagnostic value. J Nucl Med 40:371–375
14. Jacobson AF, Senior R, Cerqueira MD, Wong ND, Thomas GS, Lopez VA, Agostini D, Weiland F, Chandna H, Narula J, ADMIRE-HF Investigators (2010) ADMIRE-HF investigators. Myocardial iodine-123 meta-iodobenzylguanidine imaging and cardiac events in heart failure. Results of the prospective ADMIRE-HF (AdreView myocardial imaging for risk evaluation in heart failure) study. J Am Coll Cardiol 55:2212–2221
15. Kiyono Y, Kanegawa N, Kawashima H, Iida Y, Kinoshita T, Tamaki N, Nishimura H, Ogawa M, Saji H (2002) Age-related changes of myocardial norepinephrine transporter density in rats: implications for differential cardiac accumulation of MIBG in aging. Nucl Med Biol 29:679–684
16. Kiyono Y, Kanegawa N, Kawashima H, Fujiwara H, Iida Y, Nishimura H, Saji H (2003) A new norepinephrine transporter imaging agent for cardiac sympathetic nervous function imaging: radioiodinated (R)-N-methyl-3-(2-iodophenoxy)-3-phenylpropanamine. Nucl Med Biol 30:697–706
17. Kusmic C, Morbelli S, Marini C, Matteucci M, Cappellini C, Pomposelli E, Marzullo P, L'Abbate A, Sambuceti G (2008) Whole-body evaluation of MIBG tissue extraction in a mouse model of long-lasting type II diabetes and its relationship with norepinephrine transport protein concentration. J Nucl Med 49:1701–1706
18. Kiyono Y, Iida Y, Kawashima H, Ogawa M, Tamaki N, Nishimura H, Saji H (2002) Norepinephrine transporter density as a causative factor in alterations in MIBG myocardial uptake in NIDDM model rats. Eur J Nucl Med Mol Imaging 29:999–1005
19. Fukumitsu N, Suzuki M, Fukuda T, Kiyono Y, Kajiyama S, Saji H (2006) Reduced ^{125}I-meta-iodobenzylguanidine uptake and norepinephrine transporter density in the hearts of mice with MPTP-induced parkinsonism. Nucl Med Biol 33:37–42
20. Kiyono Y, Kajiyama S, Fujiwara H, Kanegawa N, Saji H (2005) Influence of the polyol pathway on norepinephrine transporter reduction in diabetic cardiac sympathetic nerves: implications for heterogeneous accumulation of MIBG. Eur J Nucl Med Mol Imaging 32:438–444
21. Giorgetti A, Burchielli S, Positano V, Kovalski G, Quaranta A, Genovesi D, Tredici M, Duce V, Landini L, Trivella MG, Marzullo P (2015) Dynamic 3D analysis of myocardial sympathetic innervation: an experimental study using [^{123}I]-MIBG and a CZT camera. J Nucl Med 56(3):464–469

22. Bland JM, Altman DG (1986) Statistical methods for assessing agreement between two methods of clinical assessment. Lancet 1:307–310
23. Geis WP, Kaye MP (1968) Distribution of sympathetic fibers in the left ventricular epicardial plexus of the dog. Circ Res 23:165–170
24. Pierpont GL, DeMaster EG, Reynolds S, Pederson J, Cohn JN (1985) Ventricular myocardial catecholamines in primates. J Lab Clin Med 106:205–210
25. Tsuchimochi S, Tamaki N, Tadamura E, Kawamoto M, Fujita T, Yonekura Y, Konishi J (1995) Age and gender differences in normal myocardial adrenergic neuronal function evaluated by iodine-123-MIBG imaging. J Nucl Med 36(6):969–974
26. Morozumi T, Kusuoka H, Fukuchi K, Tani A, Uehara T, Matsuda S, Tsujimura E, Ito Y, Hori M, Kamada T, Nishimura T (1997) Myocardial iodine-123-metaiodobenzylguanidine images and autonomic nerve activity in normal subjects. J Nucl Med 38(1):49–52
27. Yoshinaga K, Tomiyama Y, Manabe O, Kasai K, Katoh C, Magota K, Suzuki E, Nishijima KI, Kuge Y, Ito YM, Tamaki N (2014) Prone-position acquisition of myocardial ^{123}I-metaiodobenzylguanidine (MIBG) SPECT reveals regional uptake similar to that found using (11)C-hydroxyephedrine PET/CT. Ann Nucl Med 28:761–769
28. Schwaiger M, Kalff V, Rosenspire K, Haka MS, Molina E, Hutchins GD, Deeb M, Wolfe E, Wieland DM (1990) Noninvasive evaluation of sympathetic nervous system in human heart by positron emission tomography. Circulation 82:457–464
29. Ko BH, Paik JY, Jung KH, Bae JS, Lee EJ, Choe YS, Kim BT, Lee KH (2008) Effects of anesthetic agents on cellular [^{123}I]-MIBG transport and in vivo [^{123}I]-MIBG biodistribution. Eur J Nucl Med Mol Imaging 35:554–561